ORIGINAL ARTICLE

Extraction and characterization of novel cellulosic fiber from *Jatropha integerrima* plant stem for potential reinforcement in polymer composites

A. Felix Sahayaraj[1] · M. Tamil Selvan[1] · I. Jenish[2] · M. Ramesh[1]

Abstract

The present work attempts to discover the alternative for the synthetic fibers due to increased demand of environment-friendly materials. In order to accomplish this, a detailed characterization of novel fibers extracted from the *Jatropha integerrima* plant stems was conducted. In order to check the fiber reinforcement potentials, various properties such as chemical composition, tensile testing, water absorption, thermal stability, fiber roughness, and morphology were evaluated. The characterization results revealed important properties of *Jatropha integerrima* fiber (JIF). The fiber composition analysis indicated a cellulose content of $75.3 \pm 2.4\%$, hemicellulose content of $7.84 \pm 0.4\%$, and lignin content of $7.63 \pm 0.2\%$. This composition provides insights into the fiber's chemical makeup and its potential for various applications. The crystallinity index (CI) of JIF was determined to be 57.14%, indicating a well-defined crystalline structure. This crystallinity is important for understanding the fiber's properties and its behavior in composite materials. The fiber also demonstrated excellent thermal stability, as evidenced by its ability to endure temperatures up to 395 °C based on thermogravimetric experiments. This high-temperature resistance makes JIF suitable for applications where heat resistance is crucial. The functional groups present in the fiber were identified using Fourier transform infrared spectroscopy (FTIR), providing further information about its chemical characteristics. The tensile strength of JIF was found to be 326.7 ± 6.9 MPa, with a strain rate of $2.6 \pm 0.2\%$, highlighting its mechanical properties and potential as a reinforcement material. The scanning electron microscope (SEM) analysis revealed significant surface roughness, which can have implications for fiber-matrix interactions and the bonding in composite materials. Overall, these characterization results provide a comprehensive understanding of JIF's composition, crystallinity, thermal stability, mechanical properties, and surface morphology. The practical applications of JIF extend to a wide range of industries, including construction, automotive, aerospace, and packaging.

Keywords *Jatropha integerrima* stem fiber · FTIR · XRD · SEM · Water absorption · Chemical composition

1 Introduction

The rising demand for innovative materials among the industries increase the attention of researchers to work on novel material with environment-friendly aspects [1–3]. Natural fibers are one among these materials, which are naturally sourced and biodegradable [4, 5]. Natural fibers obtained from plants can substitute synthetic fibers in terms of lower cost, availability, and renewability [6]. Researchers all across the globe are interested in adopting less expensive and more ecologically friendly materials in order to eradicate pollution, and besides, it helps to give benefits to society [7]. Researchers are more curious to work on natural fibers due to its unique properties, such as being lightweight and non-toxic. Furthermore, it possesses various benefits such as strong thermal stability, lower density, low cost, broad availability, good strength, recyclability, and biodegradability.

The extraction of plant fibers involves obtaining fibers from different parts of plants through methods like retting or mechanical separation. After extraction, the fibers undergo preparation steps, including cleaning and drying, to remove

✉ A. Felix Sahayaraj
go2feli@gmail.com

1 Department of Mechanical Engineering, KIT-Kalaignarkarunanidhi Institute of Technology, 641402, Coimbatore, Tamil Nadu, India

2 Department of Applied Mechanics, Seenu Atoll School, Hulhu-Medhoo, Addu City 19060, Maldives

impurities and improve their handling. The processed plant fibers are then combined with a polymer matrix through techniques like compression molding, injection molding, or extrusion to create composite materials. The specific extraction, preparation, and processing methods can vary based on the type of plant fiber and intended application, ensuring that the fibers are properly prepared and integrated into the composite for optimal performance [8, 9]. Natural fiber can be derived from the stems and roots of plants such as *Grevia tiliifolia*, *Luffa cylindrica*, *Agave cantla* and *Cissus quadrangularis* is feasible according to Manimekalai et al. [10]. Furthermore, significant fiber production requires the availability of fibrous plants also a key factor. Lignocellulosic fibers offer environmental sustainability, lower carbon footprint, and biodegradability, making them useful in replacing synthetic fibers. Additionally, they promote health and safety and contribute to a circular economy by utilizing agricultural and forestry by-products [11].

The potentials of natural fiber reinforced polymer composites vary according to the resin, type of fiber, and fiber matrix adhesion. As a result, it is vital to identify novel bio fibers that allow for easy and cost-effective extraction techniques without compromising fiber characteristics. Pineapple, hemp, kenaf, banana, jute, kenaf, oil palm, snake grass, abaca, flax, ramie, luffa, sisal, and hemp have already been shown to replace synthetic fibers in a variety of uses [12]. Therefore, in the area of materials research, the identification of new bio fibers and the manufacture of composites using these fibers are important, especially for eco-friendly products. The fiber's chemical, physical, tensile, and thermal qualities essentially determine the performance of natural fiber composites. Important aspects of natural fibers for composites include their mechanical properties (strength, stiffness, toughness), morphology (aspect ratio, diameter, alignment), and surface characteristics (compatibility with polymer matrix). These aspects impact the overall performance, behavior, and durability of the composite material [13–15].

Characterizing novel natural fibers is crucial to understand their properties, such as mechanical strength, thermal stability, moisture absorption, and dimensional stability. This information is essential for determining the fiber's suitability for specific applications and assessing its compatibility with different polymer matrices. Characterization also aids in optimizing the fiber-matrix interface and identifying any potential challenges or limitations, enabling researchers and manufacturers to make informed decisions about the incorporation of these fibers into composite materials [16]. For that reason, investigations into new fiber characterization are important before utilizing fibers in composite preparation. The potential of *Jatropha integerrima* plant stem fibers as a viable alternative, considering their unique properties and abundance as a byproduct of *Jatropha* cultivation. To characterize the *Jatropha integerrima* fiber, we conducted physical and chemical analyses, FTIR, XRD, water absorption, TGA, 3D-profilometer, SEM, and a single fiber tensile test.

2 Materials

2.1 Jatropha integerrima plant

According to studies, the majority of plants in the family *Euphorbiaceae* have high fiber content. *Jatropha integerrima* plant is native to Cuba. *Jatropha integerrima* is an evergreen shrub or small tree with glossy leaves and clusters of star-shaped red, pink, or vermilion flowers. The plant has a rounded or narrow dome shape and can grow up to 15 feet in height and 10 ft in area. *Jatropha integerrima* often grows as a shrub with many slender stems but can be pruned into a single stem. The leaves length is approximately up to 7 in. They can be entire, elliptical, or oval in shape, fiddle-shaped, or have three sharp-pointed flaps. The leaves were bronze when young and brown at the base. The flowers are approximately 2.5 cm across and in clusters, with many flowers at the ends of the branches, almost year-round.

2.2 Extraction of fiber

Jatropha integerrima was cultivated in Vellakalpatti village, Salem district, Tamil Nadu, India, as shown in Fig. 1a and b. The JI plant stems are shown in Fig. 1c. For fiber separation, the JI plant stems were immersed in water for 15 days for the retting process, as shown in Fig. 1d. Once the skin decomposed, the fibers were manually removed from the stem. It was then sun-dried at ambient temperature to reduce the moisture content [17]. The extracted JIFs were shown in Fig. 1e.

3 Experimental methods

3.1 Chemical analysis

This investigation aimed to assess chemical compositions of the extracted fiber's namely lignin, cellulose, hemicellulose, ash, wax, and moisture contents. Lignin content was determined using the Klason technique. The materials were crushed and extracted with dichloromethane before hydrolysis in a 72% sulfuric acid solution. Lignin, the sole insoluble component, was isolated from the fiber and quantified. The cellulose content was determined using the Kurshner and Hoffer technique. The samples were then crushed and extracted using dichloromethane. The wax content was obtained using the Conrad technique, and the ash content was calculated according to ASTM E1755-01 [18]. For all experiments, five sets of samples were selected to ensure the accuracy of the results.

Fig. 1 a *Jatropha integerrima* plant. **b** *Jatropha integerrima* stem. **c** Microbial degradation technique. **d** *Jatropha integerrima* fiber extraction process. **e** Extracted *Jatropha integerrima* fiber

3.2 Density measurement

Density is essential for fiber characterization because the focused application is a lightweight material. The cross-sectional size of the JIF was measured using a Carl Zeiss Optical microscope. The diameter is not even in all positions; it also varies from fiber to fiber based on cross section. Thus, 20 samples were randomly selected for the experiment and the average value was recorded. The measurement was performed at various positions of the different fibers, and the mean diameter was taken for the study. Then, the density was calculated using a pycnometer with a toluene solution [19].

3.3 XRD analysis

The crystalline structure of JIF was determined using XRD. It also Provides different phases of crystalline substances present in the fiber. Powder samples were used in the experiment. An X' Pert Pro diffractometer was used for this experiment. Equation 1 was used to determine the crystalline index (CI) of the JI fiber.

$$CI = \frac{H22.57 - H18.17}{H22.57} \tag{1}$$

The crystallite size (CS) was calculated from the diffraction pattern of the cellulose [200] lattice planes. Using Scherrer's formula, the crystallite size (CS) was estimated using the following Eq. 2:

$$CS = \frac{K\lambda}{\beta \, COS\theta} \tag{2}$$

K 0.89 is Scherrer's constant.
B   Whole width of the peak at half maximum.
λ Wavelength of the radiation
θ Bragg angle

3.4 FTIR analysis

FTIR is a cost-effective, quick, and nondestructive method for confirming natural fibers functional groups. The spectra of the JIFs were obtained using a SHIMADZU MIRacle 10 spectrometer. The JIFs were ball-milled into a fine powder,

combined with KBr, and compacted into plates for FTIR analysis. The FTIR spectrum of the sample was obtained in the wavelength region of 4000–500 cm^{-1} using a range of 4 cm^{-1} resolution.

3.5 TGA analysis

For high-temperature applications, the thermal stability of natural fibers must be examined. A thermogravimetric analyzer was used to determine the thermal stability of the JIFs; the experiment was carried out in an inert gas environment (nitrogen) with a gas flow rate of 20 mL/min and a heating rate of 10 °C/min from 30 to 1000 °C. The analyzer had a heater, and the specimen was placed in an aluminum crucible with a top cover supported by a precise balance.

3.6 Tensile properties

To determine the single-fiber tensile strength, ASTM D3822 was used. It is a standard method for determining tensile characteristics (tensile strength, Young's modulus, and percentage elongation. An INSTRON 5500R Universal Testing Machine was used to conduct a single fiber tensile test of the JIF. The gauge length was maintained at 50 mm for all the trials, and 25 samples were used for the experiment. Finally, the mean value was used for analysis. The testing was carried out at a fixed cross-head speed of 0.1 mm/min and a room temperature of approximately 25 °C [20].

3.7 Moisture content measurement

The water saturation level during the immersion of JIFs was computed in percentage using Eq. 3. Selected samples were dried for 2 h in an oven at temperature range of 60–80 °C. The samples (JIFs) were then immersed in water. Weight gain was calculated periodically. The samples were rubbed with a cloth before the weight was calculated. The weights before and after immersion were substituted into the formula to determine the absorption percentage [21].

$$\text{Water absorption (\%)} = \frac{Wt - Wo}{Wt} \times 100 \qquad (3)$$

Wt Weight of the fiber after immersion.
Wo Weight of the fiber before immersion.

3.8 SEM analysis

From the SEM investigation of a single fiber, the fiber surface roughness, cracks, and grooves were examined. The surface morphology of the JIFs was studied using a scanning electron microscope (SEM, TESCAN VEGA3, Czech Republic). The surface morphology was studied at different magnifications, and the findings are presented. The experiments were effective with an accelerating voltage of 10.00 kV in a vacuum.

3.9 Roughness measurement

A computerized profilometer was used to determine the roughness of the JIFs. The fibers were randomly selected for this experiment. The machine used for this experiment was a Zeta-20 Optical 3D-Profilometer. The machine was operated in 200 steps, with a step size of 1.082 μm. The machine provides a Zeta-20 image, surface analysis, and surface skewness of the fiber surface.

4 Results and discussion

4.1 Discussion on physical and chemical analysis of JIFs

Natural fibers, as reinforcing materials, have the benefit of lower weight usage owing to their properties. The weight of the material is directly proportional to the density of the lignocellulosic reinforcement when the density measures the physical attributes. At room temperature, JIFs fiber has a density of 0.98 g/cm^3, signifying that it is appropriate for flyweight usage. The elemental analysis statistics are shown in Fig. 2. Plant growth, soil type, growing environment, and extraction process all influence chemical characterization. Chemical examination indicated that cellulose makes up $75.3 \pm 2.4\%$, hemicellulose $7.84 \pm 0.4\%$, lignin $7.61 \pm 0.2\%$, wax 1.2%, ash 3.03%, and moisture content $5.12 \pm 0.4\%$. Similar findings were reported by [22] shown in Table 1.

4.2 Discussion on FTIR analysis of JIFs

The FTIR results provided directions for finding the functional group for the respective vibrating wavenumber cm^{-1} with respect to transmittance. FTIR spectrum of JIFs is shown in Fig. 3. The results revealed that in the single bond region 4000 to 2500 cm^{-1}, vibrations exist at 3603.3 cm^{-1}, which are assigned to alcohol and hydroxyl compounds of phenols and OH stretching in the range (3640–3530 cm^{-1}). Consecutive record findings at 350.73 cm^{-1} were assigned to dimeric OH stretching in the range of (3550–3450 cm^{-1}). Vibrations did not exist in the triple-bond region from 2500 to 2000 cm^{-1}. In the double bond region from 2000 to 15,000 cm^{-1}, vibration exists at 1743.65 cm^{-1}, which was assigned to the carbonyl compound of alkyl carbonate in the range 1760–1740 cm^{-1}. Consecutive vibration was recorded at 1689.62 cm^{-1}, which was assigned to quinone or
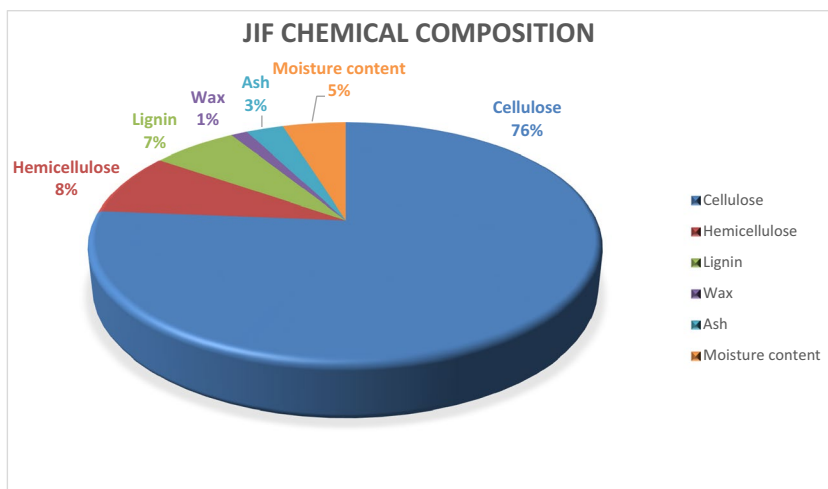
Fig. 2 Chemical composition
of JIF

Table 1 Validate the physicochemical results with others novel natural fibers

Name of the novel fiber	Cellulose (%)	Hemicellulose (%)	Lignin (%)	Wax (%)	Ash (%)	Moisture uptake (%)	Density (g/cc)	References
Jatropha inte-gerrima	75.3 ± 2.4	7.84 ± 0.4	7.61 ± 0.2	1.2	3.03	5.12 ± 0.4	0.98	Current study
Himalayacala-mus falconeri	72.5	12.7	7.76	0.14	-	6.9	1.3	[23]
Furcraea selloa K. Koch	71.13	11.6	6.9	-	-	-	1.12	[24]
Abutilon indicum	56.12	14.26	16.21	0.38	10.21	8.75	0.17	[25]
Abelmoschus ficulneus	80.86	13.4	11.23	-	-	-	-	[26]
Purple Bauhinia	60.54 ± 4.31	9.17 ± 3.45	16.27 ± 6.15	1.28 ± 0.24	6.24 ± 2.87	10.54 ± 2.25	1.46	[27]

Fig. 3 FTIR analysis of JIF
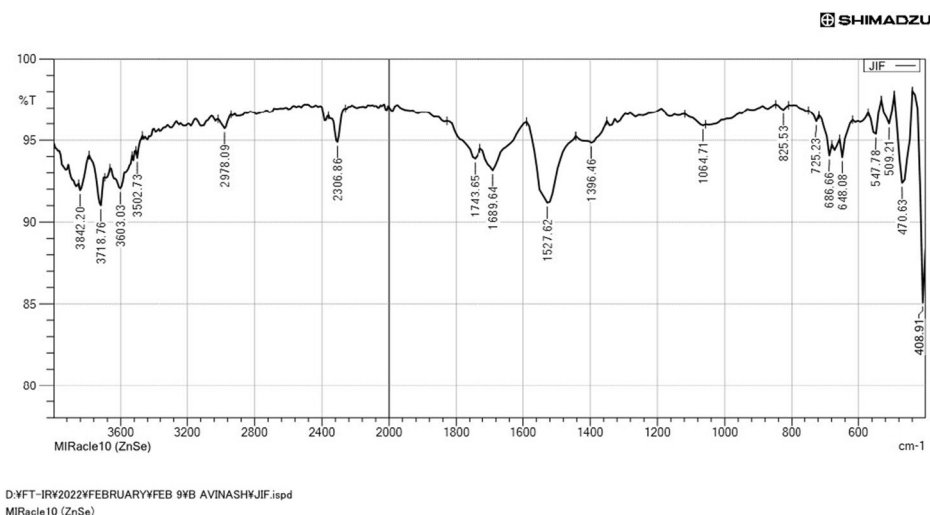
conjugated ketone in the 1690–1675 cm^{-1}. The next wavenumber exists at 1527.62 cm^{-1}, assigned to simple hetero–oxy compounds of aromatic nitro compounds from 1555 to 1485 cm^{-1}. The last vibration in the double bond region exists at 1396.46 cm^{-1}, assigned to common inorganic ions of ammonium ions in 1430–1390. The fingerprint region ranged from 1500 to 500 cm^{-1}. The vibrations at 1064.71 cm^{-1} were assigned to ether

and oxy compounds associated with alkyl-substituted ether and C-O stretch bonds. The next wavenumber was found at 825.53 cm^{-1}, assigned to the aromatic ring (aryl) of the aromatic C-H out-of-plane bend. A vibration followed this at 725.23 cm^{-1}, which revealed that the aliphatic organ halogen compound of aliphatic chloro compounds-CI stretch bond. The next wavenumber exists at 686.66 cm^{-1}, which belongs to thiols and thio-substituted compounds of disulfides (C-S stretch). The next nearby vibrations were observed at 648.08 cm^{-1}, representing the acetylenic (alkyne) alkyne C-H bend. Followed by two vibrations at consecutively 547.78 cm^{-1} and 509.21 cm^{-1}, the wavenumber represents the same functional group aliphatic organ halogen compound of aliphatic iodo compounds, C-I stretch. The last vibrations were observed in the fingerprint region at 470.63 cm^{-1}, which represent the thiols and thio-substituted compounds of polysulfides (S–S stretch). Similar findings were reported by [28]. Table 2 shows the various functional groups present in the fiber.

4.3 Discussion on XRD analysis of JIFs

The XRD results are shown in Fig. 4, where $H_{22.57}$ and $H_{18.17}$ are the intensities of the peaks at $2\theta = 22.570$ and 18.170, respectively. The iconic peak at $2\theta = 32.2720°$ showed a height of 29.72 cts, with a full-width half-maximum (FWHM) at $2\theta = 0.4896$ and d-spacing of 2.77167 Å. The XRD graph of JIFs was shown in Fig. 4. The JIF crystallinity index was determined as 57.14% using the Segal equation. In a chemical condition setting and a moisture-content environment, the crystallinity result demonstrated an optimal structure to be employed
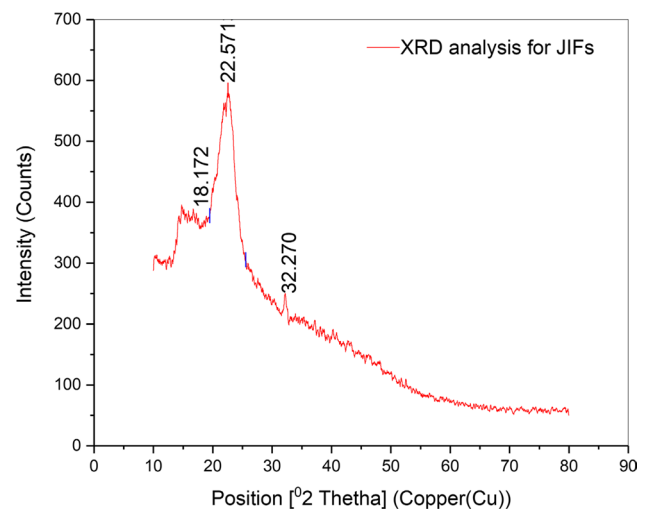

Fig. 4 XRD analysis of JIF

in biocomposites. The study by Manimaran et al. [43] investigated the XRD analysis of *Furcraea foetida* (FF) natural fibers. They observed a well-defined crystalline peak of FF at 2θ diffraction angles of 15° (1 1 0) and 22.63° (2 0 0), corresponding to cellulose-I and cellulose-IV, respectively. These findings are similar to the XRD results obtained in the current study on JIFs. The specific angles and corresponding crystalline phases may differ between FF and JIFs, the presence of well-defined peaks indicates the crystalline nature of both fiber types. Therefore, the similarity in the XRD findings suggests that JIFs, like FF, possess a crystalline structure, which contributes to their physicochemical properties and potential applications in various composites.

Table 2 Functional groups of JIF

S.no	Vibration range (wave-number cm^{-1})	Assignment	Description with wavenumber cm^{-1}	References
1	3603.03	Alcohol and hydroxyl compound	Phenols, OH stretch in range 3640–3530	[29]
2	3502.73	Alcohol and hydroxyl compound	Dimeric OH stretch 3550–3450	[30]
3	1743.65	Carbonyl compound	Alkyl carbonate 1760–1740	[31]
4	1689.64	Carbonyl compound	Quinone or conjugated ketone 1690–1675	[32]
5	1527.62	Simple hetero–oxy compounds	Aromatic nitro compounds 1555–1485	[33]
6	1396.46	Common inorganic ions	Ammonium ion 1430–1390	[34]
7	1064.71	Ether and oxy compound	Alkyl-substituted ether, C-O stretch	[35]
8	825.53	The aromatic ring (aryl)	Aromatic C-H out-of-plane bend	[36]
9	725.23	Aliphatic organohalogen compound	Aliphatic chloro compounds, C-CI stretch	[37]
10	686.66	Thiols and thio-substituted compounds	Disulfides (C-S stretch)	[38]
11	648.08	acetylenic (alkyne)	Alkyne C-H bend	[39]
12	547.78	Aliphatic organohalogen compound	Aliphatic iodo compounds, C-I stretch	[40]
	509.21			[41]
13	470.63	Thiols and thio-substituted compounds	Polysulfides (S–S stretch)	[42]

4.4 Discussion on TGA analysis of JIFs

The temperature deterioration of the JIFs was investigated using thermogravimetric analysis (TGA). The thermal degradation of JIFs is shown in Fig. 5. At 92.6 °C, the initial mass loss is caused by hydration evaporation from the JIFs. Thermal disintegration of hemicellulose was associated with a moderate thermal peak at 227 °C, with a weight reduction of 19.3%. The thermal reduction of cellulose resulted in a significant maximum temperature of almost 395 °C and a weight loss of 36.2%. At temperatures above 540 °C, ash was formed. Because of the strong phenolic-binding interactions, the results demonstrated that JIF could endure extreme heat [42].

4.5 Discussion on tensile properties of JIFs

The yield, ultimate strength, and fracture point were estimated using tensile tests. Tensile tests determine the force required to break a specimen when it extends to its breaking point. JIFs that have strain rate of $2.6 \pm 0.2\%$ were used to determine the breaking point with a remarkable tensile strength of 326.7 ± 6.9 MPa. The calculated Young's modulus for JIFs is 7.8 MPa, and the elongation at break is 3.2. These values indicate the material's ability to resist deformation under tension and its maximum elongation before failure, respectively. These properties play a significant role in assessing the mechanical behavior and potential applications of JIFs, such as in composite materials where strength and flexibility are important considerations. Tensile properties of JIFs are shown in Fig. 6.

4.6 Discussion on SEM analysis

An SEM apparatus was used to investigate the SEM images of the external layer of the JIFs, as illustrated in Fig. 7. Figure 7a depicts a collection of fiber pictures set arbitrarily on the sample chamber to evaluate several cross-sectional views of a distinct fiber at different spots. Figure 7b depicts a cross section of a fiber, analyzing many crack-like patterns that appear as long and thin cellulose fibers over the fiber's dimensions, presumably showing that the fiber bunches are kept together. The JIF fibers have good surface characteristics such as low surface roughness, high surface area high aspect ratio. The JIF fiber is flexible and appears to have a tube structure with a diameter of approximately 319 nm. Pectin and other noncellulosic compounds connect multiple primitive strands in the orientation of their length, such as fibrils (also known as fiber cells).
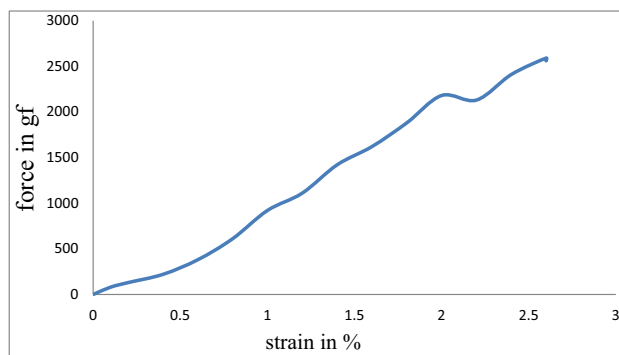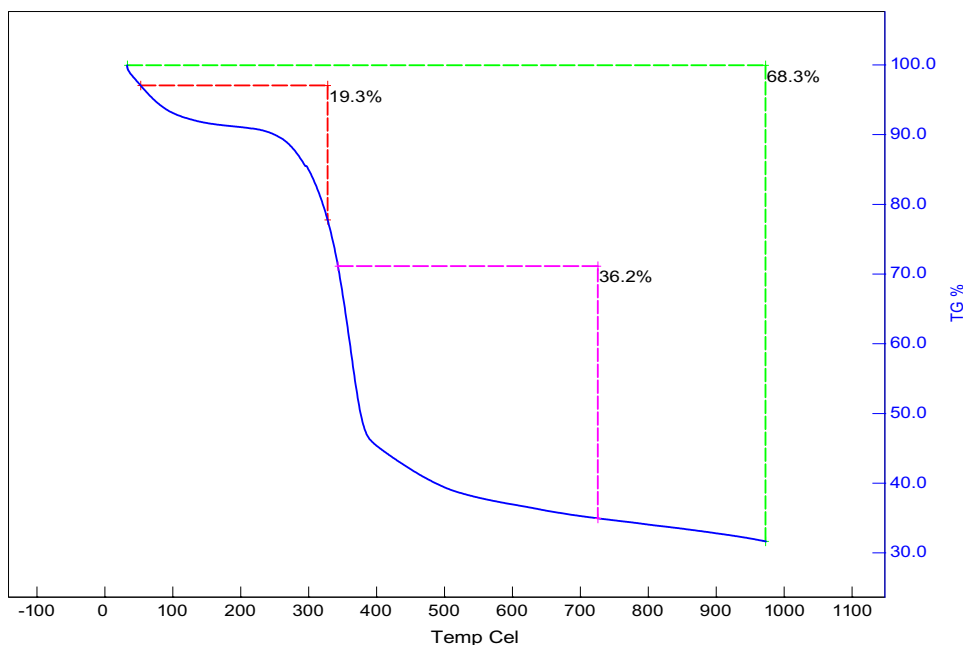
Fig. 6 Tensile properties of JIFs
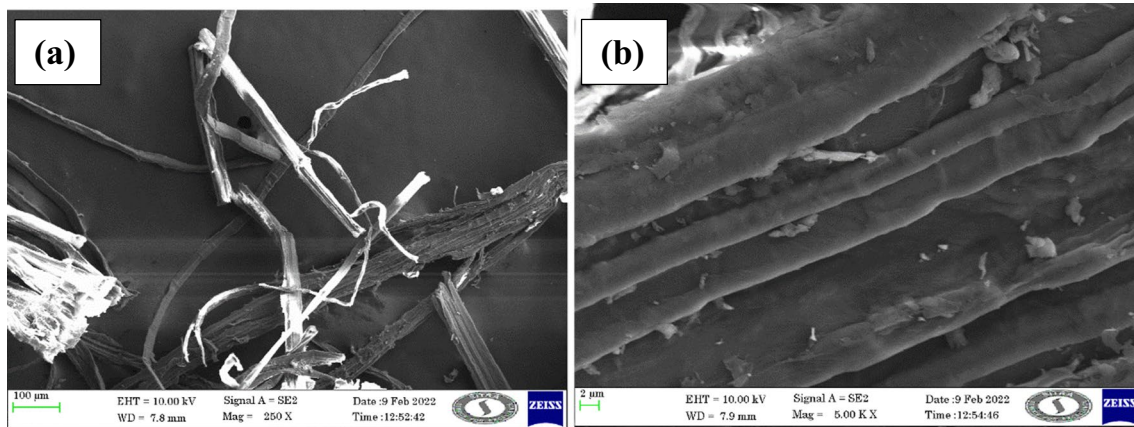
Fig. 5 TGA analysis of JIF

Fig. 7 **a** SEM analysis of JIF. **b** SEM analysis of JIF

Figure 8a depicts a massive void of fiber from a top-angle perspective, resulting in the removal of a substantial amount of cellulose from the fiber. As shown in Fig. 8b, lignin acts as a binding agent in the fiber elements by creating an adhesive bond with cellulose molecules. Natural fibers are known to have a protective covering formed by wax and pectin.

4.7 Discussion on 3D profilometer

A 3D optical profilometer was used to measure the outer-layer deviation and roughness of the JIFs. The pictures were extracted at approximately 15 μm; the *z*-axis of the picture stretched from 319 μm, and the picture step size was 1.604 μm. Roughness values of JIFs were reported in Fig. 9a.

Representations, such as Ra, Rq, and Rt, describe the roughness intensity. Rsk denotes the surface skewness, and Rku is the kurtosis number that defines the formation of the specimen height data. The skewness measurement of the profilometer was used to determine the number of peaks and valleys. The distribution of heights has been divided into two groups based on value: symmetric (Rsk = 0) and asymmetric (Rsk ≠ 0). If the Rsk coefficient is greater than zero, the peak distribution is above the normal arithmetic mean; otherwise, it is below the median. According to the data, the average Rsk value was − 0.5109, indicating that the distribution was negatively skewed. Optical interferometry of JIF is shown in Fig. 9b.

The 3D profilometer analysis revealed important surface characteristics of the JIFs. The range of view, spanning 95 × 71 μm, provided a small-scale representation of the fiber's surface. The minimum heights recorded were 73.88 μm and 128.88 μm, indicating the presence of lower points or depressions, while the maximum heights measured at 126.22 μm and 142.89 μm represented the highest elevations on the fiber's surface. The mean heights of 108.27 μm and 137.09 μm gave an average value for the overall surface height, indicating the central tendency of

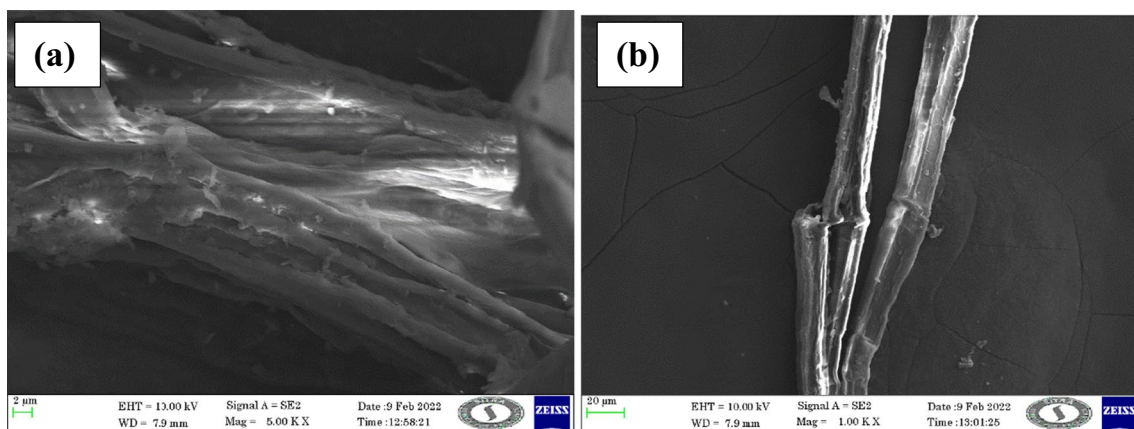**Fig. 8** **a** SEM analysis of JIF. **b** SEM analysis of JIF

Zeta Analysis Report
Image Name: Zeta Image5 File Name:
Date Acquired: Thu Feb 24 18:10:35 2022   Today: Thu Feb 24 18:10:46 2022
Z Range: 319µm No. of Steps: 200   Step Size: 1.604µm   Field of View: 95µm x 71µm

	Ra	Rq	Rpv	Rp	Rv	Rsk	Rz	Rku
	14.14	19.96	109.60	58.85	50.75	-0.2674	42.95	4.244
	9.860	13.17	83.29	28.46	54.83	-1.051	49.76	4.334
	8.950	11.35	50.94	21.76	29.18	-0.2143	32.64	2.562
Min	8.950	11.35	50.94	21.76	29.18	-1.051	32.64	2.562
Max	14.14	19.96	109.60	58.85	54.83	-0.2143	49.76	4.334
Mean	10.98	14.83	81.28	36.35	44.92	-0.5109	41.78	3.713
SD	2.264	3.705	23.99	16.14	11.25	0.3825	7.038	0.8151
Var%	20.6%	25.0%	29.5%	44.4%	25.1%	-74.9%	16.8%	22.0%

(a)
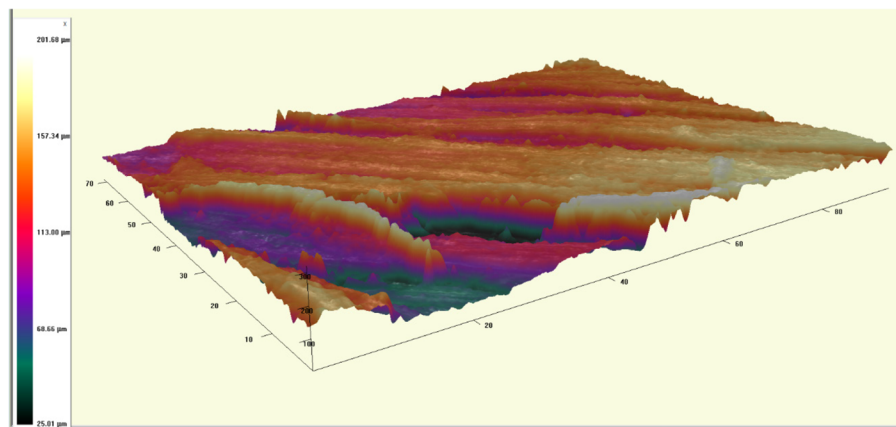
(b)
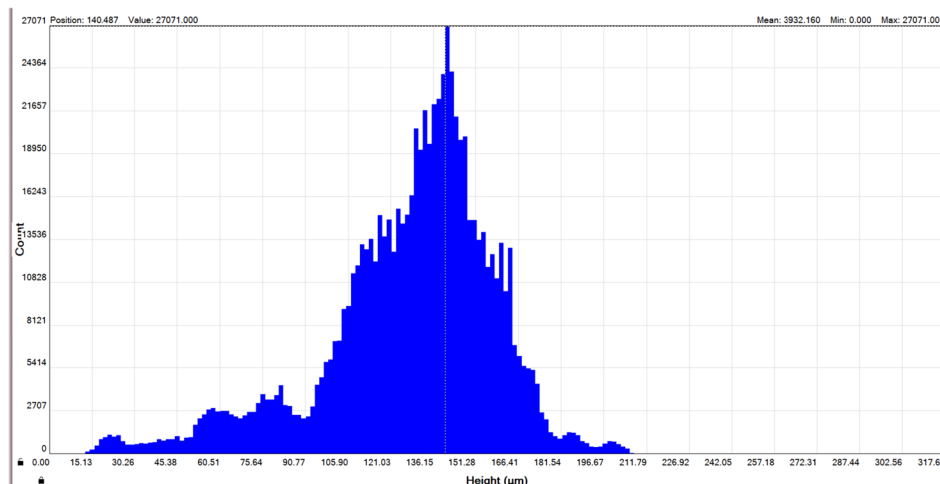
(c)

the height distribution. The standard deviation values of 24.33 µm and 5.968 µm reflected the extent of variation or dispersion in the height measurements, with higher values indicating greater variability. The variance values of 22.5% and 4.35% provided a measure of the overall spread or dispersion of the height data, indicating a wider range of height values in the dataset. These values collectively provide valuable insights into the surface topography and roughness of the JIFs, contributing to our understanding of their structural characteristics.

Picture retrieval is portrayed by an array of colors and ranges that display height. Histogram of JIF is shown in Fig. 9c. The peak height, maximum count value, and mean value of the histogram charts were 140.487 µm, 27,071 µm,

and 3932.160 μm, respectively. The vertical scale shows the number of repeats or periodicity for each peak, while the horizontal axis shows the height of the peak. The positive kurtosis histogram illustrates that the peak values are greater than the average. Because the instability in the peaks promotes the retention of the matrix with fiber, this substantial Ra value underlines the certainty of the fiber-matrix bonding.

5 Conclusions

Physicochemical features, including chemical composition, thermal stability, and tensile strength, were assessed in this study. JIFs have a tensile strength of 326.7 ± 6.9 MPa and a strain rate of $2.6 \pm 0.2\%$ because of their high cellulose content of $75.3 \pm 2.4\%$. The cellulose content is comparable to that of other commonly used biopolymer resources. It is worth noting that JIFs have a lower density of 0.98 g/cm^3 compared to other natural fibers, making them suitable for lightweight composite preparation. In addition, the moisture content was 5%. The JIF crystallinity index was calculated to be 57.14% using the Segal equation. The absorption bands of cellulose, hemicellulose, and lignin were validated by FTIR spectra at 3603.03 cm^{-1}, 1689.64 cm^{-1}, 1064.71 cm^{-1}, and 547.78 cm^{-1}, respectively. In addition, the JIFs were thermally stable at temperatures up to 395 °C. In the SEM micrographs, the exterior layer of the fibers was contaminated with environmental impurities and a noncellulosic layer. Moreover, the fiber appears to be composed of long, thin fibrils, which may imply that the fiber clusters are maintained throughout. JIFs may be used as reinforcement materials in biocomposites for many scenarios, including roof tiles, door handles, furniture panels, and decorative panels. This fiber offers great promise for manufacturing natural fiber reinforced polymer composites and studying their thermal and mechanical properties, which might lead to more innovative product development ideas.

Author contribution A. Felix Sahayaraj—conceptualization. M. Tamil Selvan—drafting. I. Jenish—visualization. M. Ramesh—supervision.

Data availability All the data were included within the article.

Declarations

Ethics approval and consent to participate Ethics approval was not applicable for this article.

Consent for publication Ethics approval was not applicable for this article.

Competing interest The authors declare no competing interests.

References

1. Saroj S, Nayak RK (2021) Improvement of mechanical and wear resistance of natural fiber reinforced polymer composites through synthetic fiber (glass/carbon) hybridization. Trans Indian Inst Met 74(11):2651–2658
2. Agarwal J, Sahoo S, Mohanty S, Nayak SK (2019) Progress of novel techniques for lightweight automobile applications through innovative eco-friendly composite materials: a review. 33(7):978–1013. https://doi.org/10.1177/0892705718815530
3. Arockiasamy FS, Muthukrishnan M (2022) Experimental investigation on the effect of fiber volume fraction of sponge gourd outer skin fiber reinforced epoxy composites. Polym Compos 43(10):6932–6942
4. Gokul K, Prabhu TR, Rajasekaran T (2017) Processing and evaluation of mechanical properties of sugarcane fiber reinforced natural composites. Trans Indian Inst Met 70(10):2537–2546
5. Gurunathan T, Mohanty S, Nayak SK (2015) A review of the recent developments in biocomposites based on natural fibres and their application perspectives. Compos Part A Appl Sci Manuf 77:1–25
6. Pradhan S, Prakash V, Acharya SK (2021) Effect of weathering on physical and mechanical characteristics of eulaliopsis binata fiber/epoxy composites. Trans Indian Inst Met 75(2):337–349
7. Alshuwaikhat HM, Abubakar I (2008) An integrated approach to achieving campus sustainability: assessment of the current campus environmental management practices. J Clean Prod 16(16):1777–1785
8. Vinod A, Sanjay MR, Suchart S, Jyotishkumar P (2020) Renewable and sustainable biobased materials: an assessment on biofibers, biofilms, biopolymers and biocomposites. J Clean Prod 258:120978
9. Sanjay MR, Siengchin S, Parameswaranpillai J, Jawaid M, Pruncu CI, Khan A (2019) A comprehensive review of techniques for natural fibers as reinforcement in composites: Preparation, processing and characterization. Carbohydr Polym 207:108–121
10. Manimekalai G, Kavitha S, Divya D, Indran S, Binoj JS (2021) Characterization of enzyme treated cellulosic stem fiber from Cissus quadrangularis plant: an exploratory investigation. Curr Res Green Sustain Chem 4:100162
11. Rangappa SM, Siengchin S, Parameswaranpillai J, Jawaid M, Ozbakkaloglu T (2022) Lignocellulosic fiber reinforced composites: progress, performance, properties, applications, and future perspectives. Polym Compos 43(2):645–691
12. Madhu P, Sanjay MR, Senthamaraikannan P, Pradeep S, Saravanakumar SS, Yogesha B (2017) A review on synthesis and characterization of commercially available natural fibers: Part II. 16(1):25–36. https://doi.org/10.1080/15440478.2017.1379045
13. Rangappa SM, Siengchin S (2022) Moving towards biofiber-based composites: Knowledge gaps and insights. Express Polym Lett 16(5):451–452
14. Singh MK, Tewari R, Zafar S, Rangappa SM, Siengchin S (2023) A comprehensive review of various factors for application feasibility of natural fiber-reinforced polymer composites. Results Mater 17:100355
15. Sanjay MR, Madhu P, Jawaid M, Senthamaraikannan P, Senthil S, Pradeep S (2018) Characterization and properties of natural fiber polymer composites: a comprehensive review. J Clean Prod 172:566–581
16. Vinod A, Sanjay MR, Siengchin S (2023) Recently explored natural cellulosic plant fibers 2018–2022: a potential raw material resource for lightweight composites. Ind Crops Prod 192:116099

17. Radzi AM, Sapuan SM, Jawaid M, Mansor MR (2019) Water absorption, thickness swelling and thermal properties of roselle/sugar palm fibre reinforced thermoplastic polyurethane hybrid composites. J Mater Res Technol 8(5):3988–3994

18. Nkapleweh AD, Tendo JF, Ebanda FB, Noah PMA, Mewoli AE, Stanislas TT (2022) Physico-chemical and mechanical characterization of triumfetta pentandra bast fiber from the equatorial region of Cameroon as a potential reinforcement of polymer composites. 19(16):13106–13119. https://doi.org/10.1080/15440478.2022.2085228

19. Kumar R, Rakesh PK, Sreehari D, Kumar D, Naik TP (2023) Experimental investigations on material properties of alkali retted Pinus Roxburghii Fiber. Biomass Convers Biorefinery 1–17

20. Ramesh M, Deepa C, Aswin US, Eashwar H, Mahadevan B, Murugan D (2017) Effect of alkalization on mechanical and moisture absorption properties of Azadirachta indica (neem tree) fiber reinforced green composites. Trans Indian Inst Met 70(1):187–199

21. Prakash V, Pradhan S, Acharya SK (2021) Tribological behavior of Syngonanthus nitens natural fiber reinforced epoxy composite. Trans Indian Inst Met 74(7):1741–1750

22. Gurukarthik Babu B, Prince Winston D, SenthamaraiKannan P, Saravanakumar SS, Sanjay MR (2018) Study on characterization and physicochemical properties of new natural fiber from Phaseolus vulgaris. 16(7):1035–1042. https://doi.org/10.1080/15440478.2018.1448318

23. Pokhriyal M, Rakesh PK, Rangappa SM, Siengchin S (2023) Effect of alkali treatment on novel natural fiber extracted from Himalayacalamus falconeri culms for polymer composite applications. Biomass Convers Biorefinery

24. Divya D, Suyambulingam I, Sanjay MR, Siengchin S (2022) Suitability examination of novel cellulosic plant fiber from Furcraea selloa K. Koch peduncle for a potential polymeric composite reinforcement. Polym Compos 43(7):4223–4243

25. ArunRamnath R et al (2023) Characterization of novel natural cellulosic fibers from Abutilon Indicum for potential reinforcement in polymer composites. Polym Compos 44(1):340–355

26. Ramalingam K et al (2022) Novel cellulosic natural fibers from Abelmoschus ficulneus weed: extraction and characterization for potential application in polymer composites. J Polym Environ 31(4):1323–1334

27. Rajeshkumar G et al (2021) Characterization of novel natural cellulosic fibers from purple bauhinia for potential reinforcement in polymer composites. Cellulose 28(9):5373–5385

28. Senthamaraikannan P, Kathiresan M (2018) Characterization of raw and alkali treated new natural cellulosic fiber from Coccinia grandis.L. Carbohydr Polym 186:332–343

29. Arifni FR, Bulan R, Sebayang F (2020) Manufacturing, characterization, and activity testing of edible film from sweet orange skin pectin (Citrus sinensis l.) with the addition of tapioca flour and glycerine as plastic. J Chem Nat Resour 2(2):97–106

30. Zhu XF, Zhang J, Chen BC (2019) Study on synthesis and thermal properties of polylactic acid. J Phys Conf Ser 1176(4):042003

31. Ramesh M, Deepa C, Rajeshkumar L, Tamil Selvan M, Balaji D (2021) Influence of fiber surface treatment on the tribological properties of Calotropis gigantea plant fiber reinforced polymer composites. Polym Compos 42(9):4308–4317

32. Prabawati SY, Yahdiyani A, Saputra Y (2021) Synthesis of the Halal fragrance compound menthyl p- anisate from fennel oil. J Phys Conf Ser 1788(1):012018

33. Popovicheva OB, Kireeva ED, Shonija NK, Vojtisek-Lom M, Schwarz J (2015) FTIR analysis of surface functionalities on particulate matter produced by off-road diesel engines operating on diesel and biofuel. Environ Sci Pollut Res 22(6):4534–4544

34. Malla KP et al (2020) Extraction and characterization of novel natural hydroxyapatite bioceramic by thermal decomposition of waste ostrich bone. Int J Biomater 2020

35. Ramesh M, Rajeshkumar L, Deepa C, Tamil Selvan M, Kushvaha V, Asrofi M (2021) Impact of silane treatment on characterization of ipomoea staphylina plant fiber reinforced epoxy composites. 19(13):5888–5899. https://doi.org/10.1080/15440478.2021.1902896

36. Raj T, Dharela R, Chauhan GS (2023) Novel method for extraction of lignin cellulose & hemicellulose from Pinus roxburghii needles. Am J Innov Sci Eng 2(1):57–68

37. Gerding H, Haring HG (1955) Raman spectra of aliphatic chlorine compounds: II. Chloroethenes and chloropropenes. Recl des Trav Chim des Pays-Bas 74(8):957–975

38. Vijay R, Vinod A, Lenin Singaravelu D, Sanjay MR, Siengchin S (2021) "Characterization of chemical treated and untreated natural fibers from Pennisetum orientale grass- a potential reinforcement for lightweight polymeric applications. Int J Light Mater Manuf 4(1):43–49

39. Raju JSN, Depoures MV, Kumaran P (2021) Comprehensive characterization of raw and alkali (NaOH) treated natural fibers from Symphirema involucratum stem. Int J Biol Macromol 186:886–896

40. Sathyamoorthy G, Vijay R, Lenin Singaravelu D (2021) Development and characterization of alkali-treated and untreated Dactyloctenium aegyptium fibers based epoxy composites. Mater Today Proc 39:1215–1220

41. Selvaraj M, Akash S, Mylsamy B (2023) Characterization of new natural fiber from the stem of Tithonia diversifolia plant. 20:(1). https://doi.org/10.1080/15440478.2023.2167144

42. Udhayakumar A, Mayandi K, Rajini N, Devi RK, Muthukannan M, Murali M (2022) Extraction and characterization of novel natural fiber from Cryptostegia grandiflora as a potential reinforcement in biocomposites. 20(1). https://doi.org/10.1080/15440478.2022.2159607

43. Manimaran P, Senthamaraikannan P, Sanjay MR, Marichelvam MK, Jawaid M (2018) Study on characterization of Furcraea foetida new natural fiber as composite reinforcement for lightweight applications. Carbohydr Polym 181:650–658